Original Contribution

Relationship Between Changes in the Temporal Dynamics of the Blood-Oxygen-Level-Dependent Signal and Hypoperfusion in Acute Ischemic Stroke

Ahmed A. Khalil, MBBS, PGDip, MSc; Ann-Christin Ostwaldt, PhD; Till Nierhaus, Dr.rer.medic, Dipl.-Ing.(FH); Ramanan Ganeshan, MD; Heinrich J. Audebert, MD; Kersten Villringer, MD; Arno Villringer, MD; Jochen B. Fiebach, MD

Background and Purpose—Changes in the blood-oxygen-level-dependent (BOLD) signal provide a noninvasive measure of blood flow, but a detailed comparison with established perfusion parameters in acute stroke is lacking. We investigated the relationship between BOLD signal temporal delay and dynamic susceptibility contrast magnetic resonance imaging (DSC-MRI) in stroke patients.

Methods—In 30 patients with acute (<24 hours) ischemic stroke, we performed Pearson correlation and multiple linear regression between DSC-MRI parameters (time to maximum [Tmax], mean transit time, cerebral blood flow, and cerebral blood volume) and BOLD-based parameters (BOLD delay and coefficient of BOLD variation). Prediction of severe hypoperfusion (Tmax >6 seconds) was assessed using receiver–operator characteristic (ROC) analysis.

Results—Correlation was highest between Tmax and BOLD delay (venous sinus reference; time shift range 7; median r=0.60; interquartile range=0.49–0.71). Coefficient of BOLD variation correlated with cerebral blood volume (median r= 0.37; interquartile range=0.24–0.51). Mean R^2 for predicting BOLD delay by DSC-MRI was 0.54 (SD=0.2) and for predicting coefficient of BOLD variation was 0.37 (SD=0.17). BOLD delay (whole-brain reference, time shift range 3) had an area under the curve of 0.76 for predicting severe hypoperfusion (sensitivity=69.2%; specificity=80%), whereas BOLD delay (venous sinus reference, time shift range 3) had an area under the curve of 0.76 (sensitivity=67.3%; specificity=83.5%).

Conclusions—BOLD delay is related to macrovascular delay and microvascular hypoperfusion, can identify severely hypoperfused tissue in acute stroke, and is a promising alternative to gadolinium contrast agent–based perfusion assessment in acute stroke.

Clinical Trial Registration—URL: http://www.clinicaltrials.gov. Unique identifier: NCT00715533 and NCT02077582.
(***Stroke***. **2017;48:00-00. DOI: 10.1161/STROKEAHA.116.015566.**)

Key Words: blood volume ■ BOLD delay ■ brain ■ gadolinium ■ perfusion imaging ■ stroke

Low-frequency oscillations (LFOs) in the blood-oxygen-level-dependent (BOLD) signal on resting-state functional magnetic resonance imaging (rsfMRI) reflect the hemodynamic sequelae of neural[1] and cardiac/respiratory[2,3] activities. The latter component, referred to as systemic LFOs, occurs with different time delays in different brain regions[4] and potentially provides information about cerebral perfusion. A disturbance of local blood flow is reflected in these LFOs as a localized delay relative to areas of normal flow, referred to as BOLD delay or hemodynamic lag. Evidence suggests that dynamic susceptibility contrast MRI (DSC-MRI) and BOLD delay provide similar information when used to assess blood flow in healthy brain tissue.[5]

BOLD delay may be a useful, less-invasive alternative to DSC-MRI. The use of DSC-MRI is limited in both research and clinical settings because it requires the administration of intravenous contrast agent, which restricts repeated data acquisition from the same patient. Moreover, observations of gadolinium deposition in the human brain have provoked concerns about the innocuousness of some of these contrast agents.[6] A prerequisite for adopting BOLD delay as a potentially safer and more convenient alternative to DSC-MRI is investigating its possible use in pathological conditions associated with blood flow disturbances.

BOLD delay can detect hypoperfusion in acute stroke,[7,8] subacute stroke,[9] and chronic cerebrovascular disease.[8,10]

Received September 27, 2016; final revision received December 24, 2016; accepted January 24, 2017.

From the Center for Stroke Research Berlin, Charité–Universitätsmedizin Berlin, Germany (A.A.K., A.-C.O., R.G., H.J.A., K.V., J.B.F.); Department of Neurology, Max Planck Institute for Human Cognitive and Brain Sciences, Leipzig, Germany (A.A.K., T.N., A.V.); Mind, Brain, Body Institute, Berlin School of Mind and Brain, Humboldt-University, Berlin, Germany (A.A.K., A.V.); and Center for Cognitive Neuroscience Berlin (CCNB), Department of Education and Psychology, Freie Universität Berlin, Germany (T.N.).

Guest Editor for this article was Christopher L.H. Chen, FRCP.

The online-only Data Supplement is available with this article at http://stroke.ahajournals.org/lookup/suppl/doi:10.1161/STROKEAHA.116.015566/-/DC1.

Correspondence to Ahmed A. Khalil, MBBS, PGDip, MSc, Center for Stroke Research Berlin, Charité Campus Benjamin Franklin, Hindenburgdamm 30, 12200 Berlin, Germany. E-mail ahmed-abdelrahim.khalil@charite.de

Studies in acute stroke have been performed on small samples, precluding a detailed quantitative assessment of the relationship between BOLD delay and DSC-MRI in this setting. In addition, several issues have not yet been addressed. First, it is currently unknown which aspect of hypoperfusion is reflected in the delay in BOLD fluctuations. Second, as a relative measure of hemodynamic compromise, it is not known whether BOLD delay is also capable of identifying severely hypoperfused tissue. The severity of hemodynamic compromise is important in stroke, as severely compromised tissue indicates tissue at risk of infarction and already infarcted tissue. Perfusion assessment techniques should, thus, be able to differentiate mild from severely compromised tissue.[11]

In this study, we build on previous findings by investigating the relationship between BOLD delay and several perfusion parameters derived from DSC-MRI. In addition, we investigate the potential of BOLD delay for differentiating mild from severe hypoperfusion in acute ischemic stroke.

Methods

Study Design

Patients with a confirmed clinical and radiological diagnosis of ischemic stroke presenting within 24 hours of symptom onset were recruited as part of the 1000Plus (3 Tesla Stroke Medical Radiologic Technology for Examining Mismatch in 1000+; NCT00715533) and LOBI-BBB (Longitudinal MRI Examinations of Patients With Brain Ischemia and Blood Brain Barrier Permeability; NCT02077582) prospective clinical studies between January 2009 and December 2015. These studies were approved by the local ethics committee, and only patients who gave written informed consent were included.

Patients were included in this substudy if they received both a DSC-MRI and rsfMRI scan in the same session within 24 hours of stroke symptom onset and had a supratentorial infarct and visible hypoperfusion on time-to-maximum maps. Patients were excluded from all analyses if the largest displacement between 2 adjacent volumes in their rsfMRI scans exceeded 3 mm or if the mean framewise displacement across the entire scan exceeded 0.5 mm.[12]

Imaging Protocol

A stroke MRI protocol[13] was performed on a Siemens (Erlangen, Germany) Tim Trio 3 Tesla MR scanner. The sequence parameters for the rsfMRI scan were: repetition time=2300 ms, echo time=30 ms, flip angle=90°, matrix=64×64, voxel dimensions=3×3×3 mm, 1 mm slice gap, 33 slices, and 150 volumes (acquisition time=5 minutes and 50 seconds) and for DSC-MRI: repetition time=1390 ms, echo time=29 ms, flip angle=60, matrix=128×128, voxel dimensions=1.8×1.8×5 mm, 0.5 mm slice gap, 21slices and 80 volumes (acquisition time=1 minute and 58 seconds). For DSC-MRI, a bolus of 5 mL Gadovist (Gadobutrol, 1 mol/L; Bayer Schering Pharma AG, Berlin, Germany) was administered followed by a saline flush at a flow rate of 5 mL/s. The rsfMRI scan was performed before the administration of contrast agent, and patients were requested to relax, lie still, and close their eyes for the duration of the scan. No thrombolytic therapy was administered between the rsfMRI and DSC-MRI scans.

Image Processing

DSC-MRI data were analyzed using Stroketool version 2.8 (2011 Digital Image Solutions – HJ Wittsack). The arterial input function was selected by manually identifying 5 to 10 voxels in the distal branches of the middle cerebral artery contralateral to the acute infarction.[14,15] Time to maximum (Tmax), mean transit time (MTT), cerebral blood flow (CBF), and cerebral blood volume (CBV) maps were generated after block-circulant singular value decomposition deconvolution of the concentration–time curve.[16]

Processing of the rsfMRI data was performed according to Lv et al.[7] The first 3 volumes were discarded, and the data were corrected for slice timing effects and motion. The data were spatially smoothed with a 6-mm gaussian kernel, band pass filtered (0.01–0.1 Hz), and 6 head motion parameters were regressed out. Time shift analysis was performed with in-house MATLAB 9 (The MathWorks, Inc, Natick, MA) scripts. Two different reference time signals were used: the mean BOLD time series across the whole brain (BOLD delay WB) and the mean BOLD time series in the major venous sinuses (BOLD delay VS), extracted using a venous sinus template (online-only Data Supplement).

The BOLD signal time series for each voxel was cross-correlated with the reference time series in steps of repetition time (2.3 seconds). Each voxel was assigned the value of the step that yielded the highest cross-correlation between the BOLD signal in that voxel and the reference signal. Positive values indicate that the voxel's BOLD signal followed the reference signal (delay), and negative values indicate that the voxel's signal preceded the reference signal.

A preliminary analysis indicated that the number of time shifts needed for maximal cross-correlation between the 2 signals (the time shift range) was variable between patients. We, therefore, report the results from 3 different time shift ranges (3, 7, and 10 corresponding to 6.9, 16.1, and 23 seconds, respectively) for each of the reference signals.

Maps of BOLD signal coefficient of variation (CoV) were generated by dividing the SD of the BOLD signal in each voxel by its mean.

The diffusion-weighted images, perfusion maps, and BOLD delay maps were registered to a study-specific echo planar imaging template, and cerebrospinal fluid artifacts were removed (online-only Data Supplement).

Relationship Between DSC-MRI and BOLD-Based Perfusion Maps

Infarcts were delineated manually on the diffusion-weighted images by an experienced neuroradiologist using MRIcro (version 1.4; Chris Rorden). The mean values of BOLD delay, Tmax delay, MTT delay, CBF, CBV, and CoV in 156 regions of interest were extracted from the maps (online-only Data Supplement). On the basis of the findings that voxels with hemodynamic lead (LFOs in the voxel preceding those in the reference time course) show no clear relationship to blood flow,[5] we excluded these voxels from all quantitative analyses. In addition, the perfusion values in each voxel were compared across perfusion maps.

Identification of Severely Hypoperfused Tissue

Using a custom vascular territory atlas (online-only Data Supplement), voxels of Tmax delay >6 seconds within the vascular territory of each patient's acute infarct were used to create a severe hypoperfusion mask. Voxels within the same vascular territory on the MTT, CBF, CBV, CoV, and BOLD delay maps (without applying a quantitative threshold) were overlain on the binarized severe hypoperfusion mask, and a receiver–operating characteristic (ROC) analysis was performed.

Statistical Analyses

Statistical analyses were performed using MATLAB 9 and SPSS 23 (IBM Corp, Armonk, NY). For each patient, relationships between mean perfusion values in the regions of interest were assessed using Pearson correlation coefficient. Multiple linear regression was performed to assess the relationship between the DSC-MRI parameters, BOLD delay, and CoV values derived from the regions of interest for each patient.

For the voxelwise analysis, Pearson correlation was calculated between the different perfusion maps. In addition, a ROC analysis was performed to evaluate the performance of each of the perfusion maps in predicting severely hypoperfused (Tmax >6 seconds) tissue.[17] The ROC analysis was performed for each patient separately and with all voxels pooled across all patients (n=30), and the areas under the ROC curve (AUC) are reported. In the pooled analysis, optimal perfusion thresholds were determined by attributing equal weight to sensitivity and specificity.[17]

Results

Patients

Thirty patients were eligible for analysis (online-only Data Supplement). Mean age in the sample was 71 years (SD=14 years) and 17 out of 30 patients were men. Median time from symptom onset to MRI was 13 hours (interquartile range [IQR]=2.4–17.3 hours). Ten patients were scanned within 4.5 hours of symptom onset, and 15 patients received intravenous thrombolysis, 8 of these treatments were computed tomography based (before MRI). The median National Institutes of Health Stroke Scale score on admission was 4 (IQR=3–12) and at discharge was 2 (IQR=1–5).

Vascular territories of the acute infarct were distributed as follows: middle cerebral artery=21, anterior cerebral artery=2, and posterior cerebral artery=7. Median diffusion-weighted images lesion volume was 14.6 mL (IQR=5.9–28.9 mL). Twenty-three patients had a vessel occlusion on magnetic resonance angiography, and 10 patients had imaging evidence of a previous infarction.

The mean framewise displacement[12] across all image volumes ranged from 0.07 to 0.35 mm (median=0.2 mm) in the rsfMRI data and from 0.09 to 0.48 (median=0.21 mm) in the DSC-MRI data.

Relationship Between DSC-MRI and BOLD-Based Perfusion Maps

Figure 1 shows the distribution of correlation coefficients between the various DSC-MRI and BOLD delay parameters (correlations between the individual DSC-MRI parameters are shown for comparison) in the sample. The highest median correlation was between Tmax and VS7 (0.60; IQR=0.49–0.71) and between MTT and WB3 (0.50; IQR=0.20–0.81). CBF was most correlated with VS7 (−0.42; IQR=−0.58 to −0.26), and CoV was most correlated with CBV (0.37; IQR=0.24–0.51). Example perfusion maps are shown in Figure 2, and the corresponding scatter plots from the region-of-interest analysis are shown in Figure 3. There was no statistically significant relationship between the head motion metrics and the correlation coefficients of any of the pairs of DSC-MRI and BOLD-based perfusion parameters (Figure I in the online-only Data Supplement). Multiple linear regression was used to predict BOLD delay (VS7) and CoV based on Tmax, MTT, CBF, and CBV for each subject. The mean R^2 across subjects for the prediction of BOLD delay was 0.54 (SD=0.23). The mean R^2 across subjects for the prediction of CoV was 0.37 (SD=0.17). Table 1 shows the mean standardized β coefficients across the sample for the independent variables. A comparison between the R^2 values from models incorporating each of the DSC-MRI parameter maps separately, as well as combined, is shown in Figure II in the online-only Data Supplement.

The distribution of voxelwise correlation coefficients between the DSC-MRI and BOLD delay parameters can be found in Figure III in the online-only Data Supplement.

Identification of Severely Hypoperfused Tissue

In the individual ROC analysis, performed for each patient separately, the MTT map had a median AUC of 0.84 for predicting severe hypoperfusion (defined as >6 seconds). The BOLD delay map with the highest median AUC was VS3 (0.74). Table 2 shows the median and IQR of the AUCs for all the maps.

When all 30 patients were pooled, the BOLD delay maps with the highest AUC for predicting severe hypoperfusion were VS3 (0.76) and WB3 (0.76). The AUC for the MTT map was 0.86. The ROC curves for the pooled analysis are shown in Figure 4, and the optimal thresholds are shown in Table 2.

Discussion

In this study, we performed a detailed comparison between perfusion parameters extracted from the BOLD signal and hypoperfusion detected using DSC-MRI in a cohort of acute

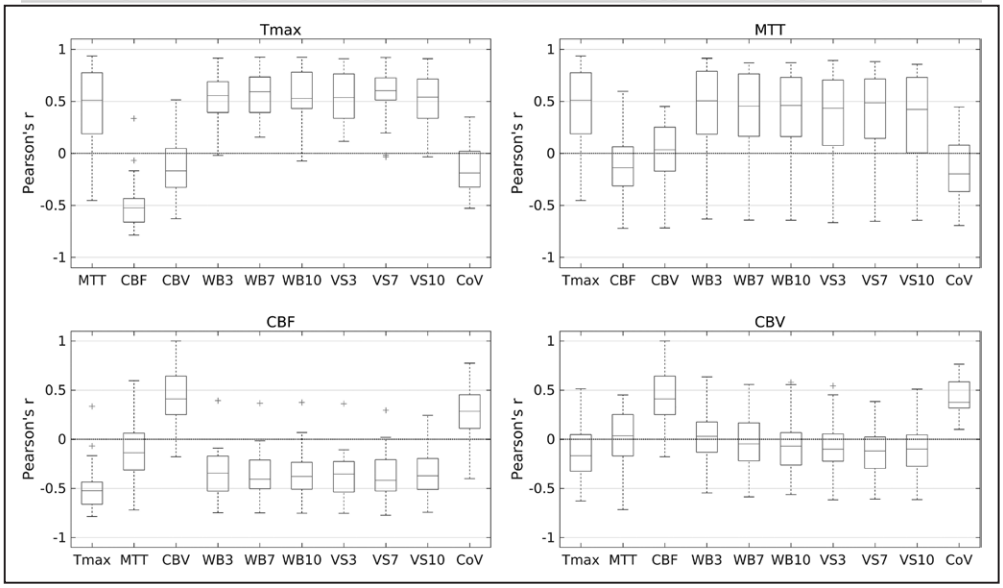

Figure 1. Boxplots of the correlation coefficients from the region of interest–based comparison of the different perfusion maps for the study sample (n=30). BOLD indicates blood oxygen level dependent; CBF, cerebral blood flow; CBV, cerebral blood volume; CoV, coefficient of variation; MTT, mean transit time; Tmax, time to maximum; VS, BOLD delay using venous reference signal; and WB, BOLD delay using whole-brain reference signal.

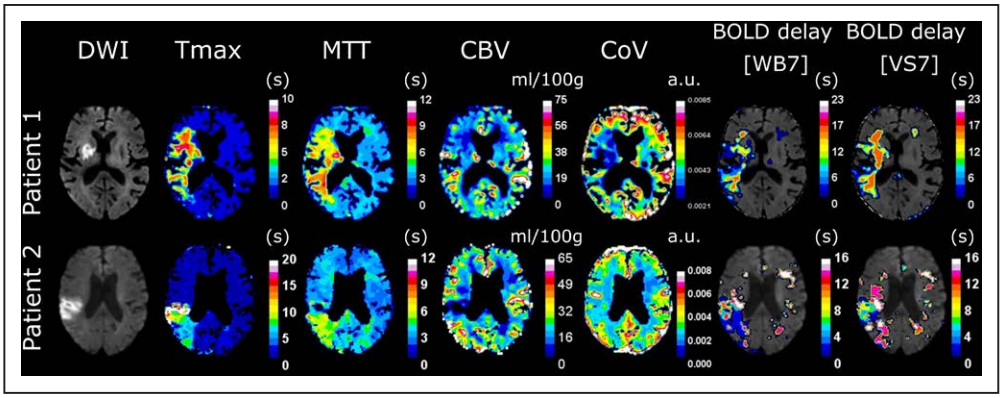

Figure 2. Diffusion-weighted images (DWI) and perfusion maps, after removal of cerebrospinal fluid artifacts, from 2 patients; one showing high correlation and the other showing moderate correlation between perfusion parameters. BOLD indicates blood oxygen level dependent; CBV, cerebral blood volume; CoV, coefficient of variation; MTT, mean transit time; Tmax, time to maximum; VS, BOLD delay using venous reference signal; and WB, BOLD delay using whole-brain reference signal.

ischemic stroke patients. Our results indicate that BOLD delay is closely related to several perfusion measures derived from DSC-MRI including Tmax, MTT, and CBF.

Although the physiological surrogate of BOLD delay is not yet known, it is believed to represent the delayed arrival in the tissue (relative to the reference region) of boluses of oxygenated blood propagated by the heart, influenced by variations in the respiratory and cardiac cycles. In DSC-MRI, this is analogous to Tmax, which is the time taken for the contrast bolus to pass from the vessel from which the arterial input function is measured to the tissue.[18] Indeed, several studies[5,10] have shown a close relationship between Tmax and BOLD delay. MTT, however, predominantly reflects microvascular perfusion.[19] The distinction between bolus arrival delay and microvascular perfusion is relevant in acute stroke because they have different effects on predicting tissue at risk of infarction.[20,21]

Some of the earliest studies on BOLD delay found spatial similarities between MTT lesions and BOLD delay lesions.[7,8] Our study shows that BOLD delay is related to both Tmax and MTT on a quantitative level. Although Tmax is the major predictor of BOLD delay, MTT predicts BOLD delay to some extent even when the influence of Tmax is adjusted for (Table 1). However, the relationship between MTT and BOLD delay shows more individual variability than that between Tmax and BOLD delay, possibly because MTT is more dependent than Tmax on the precise determination of the area under the concentration–time curve and hence the arterial input function.[22]

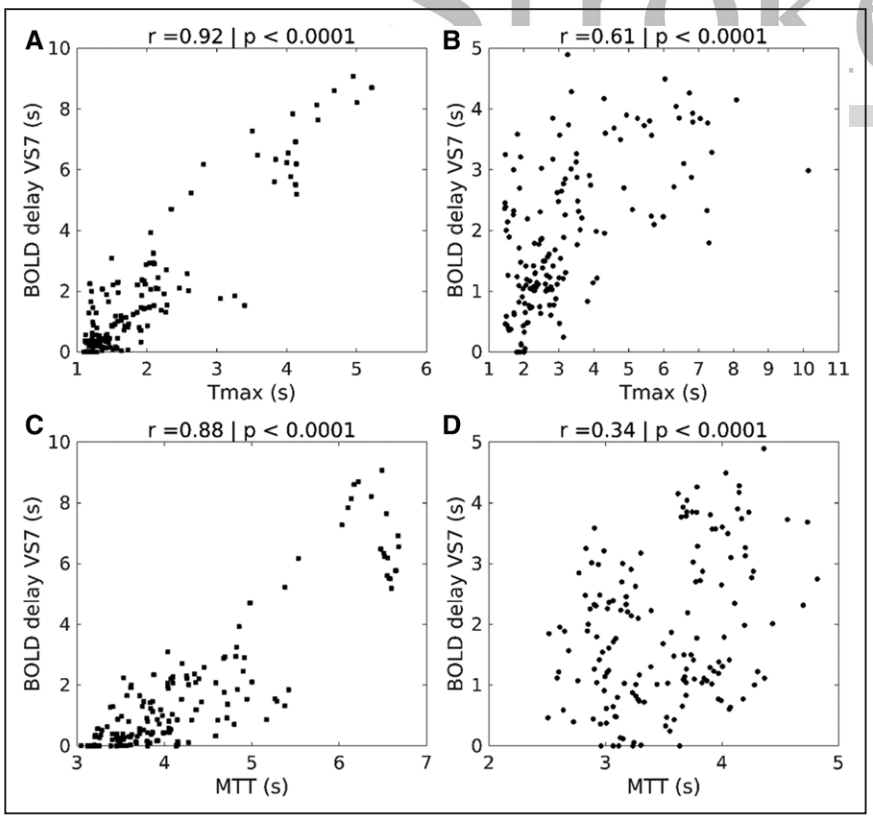

Figure 3. Scatter plots from the region-of-interest (ROI) analysis of the same 2 patients as in Figure 2. **A** and **C**, Images from patient 1. **B** and **D**, Images from patient 2. The Pearson correlation coefficient (*r*) and *P* values of the relationship between the perfusion values extracted from 156 ROIs are shown for each comparison. BOLD indicates blood oxygen level dependent; MTT, mean transit time; Tmax, time to maximum; and VS, BOLD delay using venous reference signal.

Table 1. Results of the Multiple Linear Regression Model for the Prediction of BOLD Delay (VS7) and BOLD CoV by DSC-MRI Parameter Maps

	Tmax	MTT	CBF	CBV
BOLD delay (VS7)	0.43 (0.25)	0.19 (0.33)	−0.12 (0.24)	0.03 (0.20)
CoV	0.05 (0.27)	−0.2 (0.37)	0.08 (0.40)	0.39 (0.28)

The standardized regression coefficients (β) are shown as means across the sample, with SD in parentheses. BOLD indicates blood oxygen level dependent; CBF, cerebral blood flow; CBV, cerebral blood volume; CoV, coefficient of variation; DSC-MRI, dynamic susceptibility contrast magnetic resonance imaging; MTT, mean transit time; Tmax, time to maximum; and VS, BOLD delay using venous reference signal.

Arterial spin labeling is another promising noninvasive method for assessing cerebral perfusion. In a direct quantitative comparison to DSC-MRI in 24 acute stroke patients, arterial transit time on multidelay arterial spin labeling maps was moderately correlated with Tmax (r=0.66) and MTT (r=0.59).[23] BOLD delay showed comparable correlations with DSC-MRI in our study (with Tmax, r=0.60; and MTT, r=0.50). Directly comparing the diagnostic performances of BOLD delay and arterial spin labeling for detecting hypoperfusion in acute stroke could provide useful information about their relative merits.

Arguably, the most appealing characteristic of resting-state functional MRI is that it provides multiple types of information in one scan. It has been used extensively to study functional connectivity between brain regions and more recently for blood flow assessment. In this study, we also show that it provides information about changes in blood volume. The CoV of the BOLD signal, which reflects how much the oscillations fluctuate around the mean, is moderately correlated with CBV (BOLD delay, however, is not). CBV reflects both vessel size and density,[24] the latter of which has been recently linked to systemic LFOs in the BOLD signal in healthy subjects.[25] Increased CBV in the regions surrounding an acute infarct may be a protective response suggestive of good collateral flow,[26] and its assessment, thus, potentially provides useful additional information in acute stroke.

One of the advantages of DSC-MRI is that quantitative thresholds of Tmax or MTT can help identify severe hypoperfusion that progresses to infarction without intervention (tissue at risk).[27,28] Our study found that BOLD delay severity is capable of predicting areas of severe hypoperfusion, which we defined as Tmax delay of >6 seconds, with moderate accuracy. Longitudinal studies in acute stroke patients may be able to clarify whether BOLD delay can predict tissue at risk of infarction.

The relationships between the BOLD delay and DSC-MRI parameters show substantial individual variability, which may be explained by interindividual or intraindividual differences in cardiorespiratory physiology. More importantly, however, there is marked variability between individuals in the effects of cardiac and respiratory activity on the BOLD signal.[29] Fluctuations in heart rate and blood pressure, which contribute to BOLD signal LFOs,[30] even show prominent circadian variation within the same individual.[31,32] Although motion contributes to individual variability in the results of functional MRI analyses,[33] we did not find a statistically significant relationship between motion and BOLD delay (Figure I in the online-only Data Supplement). Finally, differences in vigilance and whether the data are collected with the subjects' eyes open or closed influence neurally driven physiological delays,[34] but it is not known whether they also affect hemodynamic delays.

In its current form, there are some limitations to the BOLD delay technique. Using the venous sinus signal as a reference has shown promise in our current study and in previous reports.[10] However, it requires either manual delineation[10] or the use of a template,[5] making it inconvenient for routine clinical use. The whole-brain signal, however, is conveniently extracted, but the heterogeneity of infarcts in a typical stroke population means that this reference can cause interindividual differences in how BOLD delay is calculated. However, this is only relevant when the ischemic tissue is large,[7] which was not the case in our study sample. This limitation should nevertheless be kept in mind during routine use. In addition, because the signal-to-noise ratio of rsfMRI is lower than that of DSC-MRI, the sequence is particularly sensitive to motion, the effects of which require more extensive investigation. Finally, the temporal resolution of rsfMRI as implemented in this study is lower than DSC-MRI (2.3 compared with 1.3 seconds), and the spatial resolutions of the 2 sequences are markedly different, making their direct comparison difficult.

We are currently investigating several potential solutions for these challenges. Independent component analysis can

Table 2. Results of the ROC Analysis for the Prediction of Severe Hypoperfusion (Tmax >6 s) by the Perfusion Maps

	MTT	WB3	WB7	WB10	VS3	VS7	VS10	CBF	CBV	CoV
Individual AUC, median (IQR)	0.84 (0.71–0.9)	0.70 (0.58–0.78)	0.70 (0.57–0.77)	0.67 (0.54–0.78)	0.74 (0.59–0.77)	0.70 (0.57–0.78)	0.66 (0.55–0.74)	0.54 (0.48–0.6)	0.62 (0.55–0.66)	0.63 (0.54–0.7)
Pooled AUC	0.86	0.76	0.74	0.72	0.76	0.74	0.70	0.57	0.66	0.63
Optimal threshold	>5 s	>2.3 s	>2.3 s	>2.3 s	>2.3 s	>2.3 s	>2.3 s	<24	<15	$<3.158\times10^{-3}$
Sensitivity, %	80.2	69.2	66.1	62.6	67.3	63.2	54.0	56.1	63.7	58.4
Specificity, %	81	80	79.5	79.7	83.5	82.4	83.4	54.5	60.8	58.4

AUC indicates area under the ROC curve; BOLD, blood oxygen level dependent; CBF, cerebral blood flow; CBV, cerebral blood volume; CoV, coefficient of variation; IQR, interquartile range; MTT, mean transit time; ROC, receiver–operator characteristic; Tmax, time to maximum; VS, BOLD delay using venous reference signal; and WB, BOLD delay using whole-brain reference signal.

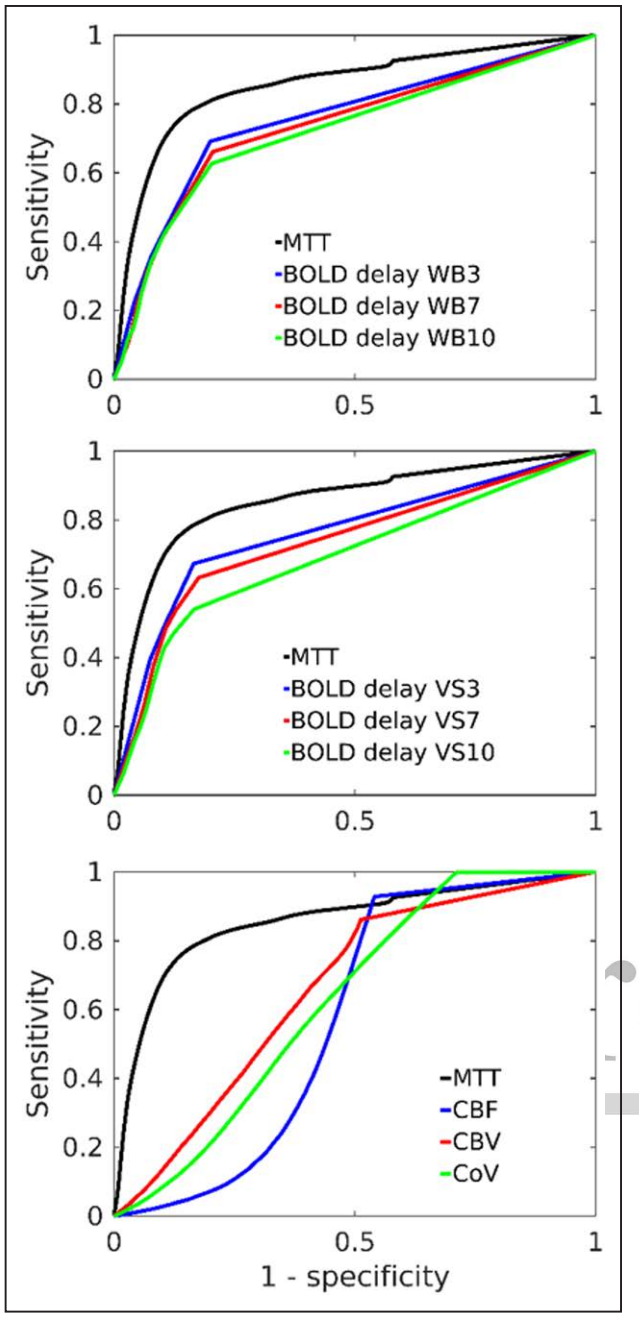

Figure 4. Receiver–operator characteristic curves of the prediction of time to maximum (Tmax) >6 s by the different perfusion maps (pooled across all subjects). BOLD indicates blood oxygen level dependent; CBF, cerebral blood flow; CBV, cerebral blood volume; CoV, coefficient of variation; MTT, mean transit time; VS, BOLD delay using venous reference signal; and WB, BOLD delay using whole-brain reference signal.

automatically extract venous time courses[35] for use as reference signals and has been applied in a similar way to detect the arterial input function in DSC-MRI.[36] It may improve the quality of the reference time course used to assess BOLD delay and has the added advantage of reducing the effects of head motion on the data.[37,38] Multiband sequences, which allow the acquisition of rsfMRI data at a high temporal resolution,[39] may be useful for a more refined assessment of hypoperfusion in acute stroke.

Conclusions

Our study confirms previous reports that cerebral hemodynamics can be noninvasively assessed using resting-state functional MRI. In acute stroke patients, BOLD delay is related to both macrovascular delay and microvascular hypoperfusion, and information about blood volume can be extracted from the variance of the BOLD signal. Our results also indicate that BOLD delay can identify severely hypoperfused tissue, although longitudinal studies are needed to verify whether this leads to accurate prediction of tissue at risk of infarction.

Sources of Funding

K. Villringer was supported by grants from the German Federal Ministry of Education and Research (01EO0801 and 01EO01301). These grants also financed the 1000plus and LOBI-BBB studies. A.A. Khalil was supported by a NeuroCure Cluster of Excellence PhD Fellowship.

Disclosures

Dr Fiebach has received consulting, lecture, and advisory board fees from Perceptive, BioClinica, Boehringer Ingelheim, Cerevast, and Brainomix. K. Villringer has received consulting fees from Parexel. The other authors report no conflicts.

References

1. Magri C, Schridde U, Murayama Y, Panzeri S, Logothetis NK. The amplitude and timing of the BOLD signal reflects the relationship between local field potential power at different frequencies. *J Neurosci*. 2012;32:1395–1407. doi: 10.1523/JNEUROSCI.3985-11.2012.
2. Tong Y, Hocke LM, Licata SC, Frederick Bd. Low-frequency oscillations measured in the periphery with near-infrared spectroscopy are strongly correlated with blood oxygen level-dependent functional magnetic resonance imaging signals. *J Biomed Opt*. 2012;17:106004. doi: 10.1117/1.JBO.17.10.106004.
3. Zhu DC, Tarumi T, Khan MA, Zhang R. Vascular coupling in resting-state fMRI: evidence from multiple modalities. *J Cereb Blood Flow Metab*. 2015;35:1910–1920. doi: 10.1038/jcbfm.2015.166.
4. Tong Y, Frederick BD. Time lag dependent multimodal processing of concurrent fMRI and near-infrared spectroscopy (NIRS) data suggests a global circulatory origin for low-frequency oscillation signals in human brain. *Neuroimage*. 2010;53:553–564. doi: 10.1016/j.neuroimage.2010.06.049.
5. Tong Y, Lindsey KP, Hocke LM, Vitaliano G, Mintzopoulos D, Frederick BD. Perfusion information extracted from resting state functional magnetic resonance imaging. *J Cereb Blood Flow Metab*. 2017;37:564–576. doi: 10.1177/0271678X16631755.
6. McDonald RJ, McDonald JS, Kallmes DF, Jentoft ME, Murray DL, Thielen KR, et al. Intracranial gadolinium deposition after contrast-enhanced MR imaging. *Radiology*. 2015;275:772–782. doi: 10.1148/radiol.15150025.
7. Lv Y, Margulies DS, Cameron Craddock R, Long X, Winter B, Gierhake D, et al. Identifying the perfusion deficit in acute stroke with resting-state functional magnetic resonance imaging. *Ann Neurol*. 2013;73:136–140. doi: 10.1002/ana.23763.
8. Amemiya S, Kunimatsu A, Saito N, Ohtomo K. Cerebral hemodynamic impairment: assessment with resting-state functional MR imaging. *Radiology*. 2014;270:548–555. doi: 10.1148/radiol.13130982.
9. Siegel JS, Snyder AZ, Ramsey L, Shulman GL, Corbetta M. The effects of hemodynamic lag on functional connectivity and behavior after stroke. *J Cereb Blood Flow Metab*. 2016;36:2162–2176. doi: 10.1177/0271678X15614846.
10. Christen T, Jahanian H, Ni WW, Qiu D, Moseley ME, Zaharchuk G. Noncontrast mapping of arterial delay and functional connectivity using resting-state functional MRI: a study in Moyamoya patients. *J Magn Reson Imaging*. 2015;41:424–430. doi: 10.1002/jmri.24558.
11. Wintermark M, Albers GW, Broderick JP, Demchuk AM, Fiebach JB, Fiehler J, et al; Stroke Imaging Research (STIR) and Virtual International Stroke Trials Archive (VISTA)-Imaging Investigators. Acute stroke

imaging research roadmap II. *Stroke*. 2013;44:2628–2639. doi: 10.1161/STROKEAHA.113.002015.
12. Power JD, Barnes KA, Snyder AZ, Schlaggar BL, Petersen SE. Spurious but systematic correlations in functional connectivity MRI networks arise from subject motion. *Neuroimage*. 2012;59:2142–2154. doi: 10.1016/j.neuroimage.2011.10.018.
13. Hotter B, Pittl S, Ebinger M, Oepen G, Jegzentis K, Kudo K, et al. Prospective study on the mismatch concept in acute stroke patients within the first 24 h after symptom onset - 1000Plus study. *BMC Neurol*. 2009;9:60. doi: 10.1186/1471-2377-9-60.
14. Calamante F. Arterial input function in perfusion MRI: a comprehensive review. *Prog Nucl Magn Reson Spectrosc*. 2013;74:1–32. doi: 10.1016/j.pnmrs.2013.04.002.
15. Ebinger M, Brunecker P, Jungehülsing GJ, Malzahn U, Kunze C, Endres M, et al. Reliable perfusion maps in stroke MRI using arterial input functions derived from distal middle cerebral artery branches. *Stroke*. 2010;41:95–101. doi: 10.1161/STROKEAHA.109.559807.
16. Wu O, Østergaard L, Weisskoff RM, Benner T, Rosen BR, Sorensen AG. Tracer arrival timing-insensitive technique for estimating flow in MR perfusion-weighted imaging using singular value decomposition with a block-circulant deconvolution matrix. *Magn Reson Med*. 2003;50:164–174. doi: 10.1002/mrm.10522.
17. Fawcett T. An introduction to ROC analysis. *Pattern Recognit Lett*. 2006;27:861–874.
18. Calamante F, Christensen S, Desmond PM, Ostergaard L, Davis SM, Connelly A. The physiological significance of the time-to-maximum (Tmax) parameter in perfusion MRI. *Stroke*. 2010;41:1169–1174. doi: 10.1161/STROKEAHA.110.580670.
19. Østergaard L. Principles of cerebral perfusion imaging by bolus tracking. *J Magn Reson Imaging*. 2005;22:710–717. doi: 10.1002/jmri.20460.
20. Olivot JM, Mlynash M, Zaharchuk G, Straka M, Bammer R, Schwartz N, et al. Perfusion MRI (Tmax and MTT) correlation with xenon CT cerebral blood flow in stroke patients. *Neurology*. 2009;72:1140–1145. doi: 10.1212/01.wnl.0000345372.49233.e3.
21. Christensen S, Mouridsen K, Wu O, Hjort N, Karstoft H, Thomalla G, et al. Comparison of 10 perfusion MRI parameters in 97 sub-6-hour stroke patients using voxel-based receiver operating characteristics analysis. *Stroke*. 2009;40:2055–2061. doi: 10.1161/STROKEAHA.108.546069.
22. Thijs VN, Somford DM, Bammer R, Robberecht W, Moseley ME, Albers GW. Influence of arterial input function on hypoperfusion volumes measured with perfusion-weighted imaging. *Stroke*. 2004;35:94–98. doi: 10.1161/01.STR.0000106136.15163.73.
23. Wang DJ, Alger JR, Qiao JX, Gunther M, Pope WB, Saver JL, et al; UCLA Stroke Investigators. Multi-delay multi-parametric arterial spin-labeled perfusion MRI in acute ischemic stroke - comparison with dynamic susceptibility contrast enhanced perfusion imaging. *Neuroimage Clin*. 2013;3:1–7. doi: 10.1016/j.nicl.2013.06.017.
24. Pathak AP, Schmainda KM, Ward BD, Linderman JR, Rebro KJ, Greene AS. MR-derived cerebral blood volume maps: issues regarding histological validation and assessment of tumor angiogenesis. *Magn Reson Med*. 2001;46:735–747.
25. Tong Y, Hocke LM, Lindsey KP, Erdoğan SB, Vitaliano G, Caine CE, et al. Systemic low-frequency oscillations in BOLD signal vary with tissue type. *Front Neurosci*. 2016;10:313. doi: 10.3389/fnins.2016.00313.
26. Cortijo E, Calleja AI, García-Bermejo P, Mulero P, Pérez-Fernández S, Reyes J, et al. Relative cerebral blood volume as a marker of durable tissue-at-risk viability in hyperacute ischemic stroke. *Stroke*. 2014;45:113–118. doi: 10.1161/STROKEAHA.113.003340.
27. Olivot JM, Mlynash M, Thijs VN, Kemp S, Lansberg MG, Wechsler L, et al. Optimal Tmax threshold for predicting penumbral tissue in acute stroke. *Stroke*. 2009;40:469–475. doi: 10.1161/STROKEAHA.108.526954.
28. Zaro-Weber O, Moeller-Hartmann W, Heiss WD, Sobesky J. Maps of time to maximum and time to peak for mismatch definition in clinical stroke studies validated with positron emission tomography. *Stroke*. 2010;41:2817–2821. doi: 10.1161/STROKEAHA.110.594432.
29. Chang C, Glover GH. Relationship between respiration, end-tidal CO2, and BOLD signals in resting-state fMRI. *Neuroimage*. 2009;47:1381–1393. doi: 10.1016/j.neuroimage.2009.04.048.
30. Mitra PP, Ogawa S, Hu X, Uğurbil K. The nature of spatiotemporal changes in cerebral hemodynamics as manifested in functional magnetic resonance imaging. *Magn Reson Med*. 1997;37:511–518.
31. Takalo R, Korhonen I, Majahalme S, Tuomisto M, Turjanmaa V. Circadian profile of low-frequency oscillations in blood pressure and heart rate in hypertension. *Am J Hypertens*. 1999;12(9 pt 1):874–881.
32. Julien C. The enigma of Mayer waves: facts and models. *Cardiovasc Res*. 2006;70:12–21. doi: 10.1016/j.cardiores.2005.11.008.
33. Lund TE, Nørgaard MD, Rostrup E, Rowe JB, Paulson OB. Motion or activity: their role in intra- and inter-subject variation in fMRI. *Neuroimage*. 2005;26:960–964. doi: 10.1016/j.neuroimage.2005.02.021.
34. Mitra A, Snyder AZ, Hacker CD, Raichle ME. Lag structure in resting-state fMRI. *J Neurophysiol*. 2014;111:2374–2391. doi: 10.1152/jn.00804.2013.
35. Tong Y, Hocke LM, Nickerson LD, Licata SC, Lindsey KP, Frederick Bd. Evaluating the effects of systemic low frequency oscillations measured in the periphery on the independent component analysis results of resting state networks. *Neuroimage*. 2013;76:202–215. doi: 10.1016/j.neuroimage.2013.03.019.
36. Calamante F, Mørup M, Hansen LK. Defining a local arterial input function for perfusion MRI using independent component analysis. *Magn Reson Med*. 2004;52:789–797. doi: 10.1002/mrm.20227.
37. Kelly RE Jr, Alexopoulos GS, Wang Z, Gunning FM, Murphy CF, Morimoto SS, et al. Visual inspection of independent components: defining a procedure for artifact removal from fMRI data. *J Neurosci Methods*. 2010;189:233–245. doi: 10.1016/j.jneumeth.2010.03.028.
38. Griffanti L, Salimi-Khorshidi G, Beckmann CF, Auerbach EJ, Douaud G, Sexton CE, et al. ICA-based artefact removal and accelerated fMRI acquisition for improved resting state network imaging. *Neuroimage*. 2014;95:232–247. doi: 10.1016/j.neuroimage.2014.03.034.
39. Tong Y, Frederick Bd. Tracking cerebral blood flow in BOLD fMRI using recursively generated regressors. *Hum Brain Mapp*. 2014;35:5471–5485. doi: 10.1002/hbm.22564.

Relationship Between Changes in the Temporal Dynamics of the Blood-Oxygen-Level-Dependent Signal and Hypoperfusion in Acute Ischemic Stroke

Ahmed A. Khalil, Ann-Christin Ostwaldt, Till Nierhaus, Ramanan Ganeshan, Heinrich J. Audebert, Kersten Villringer, Arno Villringer and Jochen B. Fiebach

Stroke. published online March 8, 2017;
Stroke is published by the American Heart Association, 7272 Greenville Avenue, Dallas, TX 75231

Print ISSN: 0039-2499. Online ISSN: 1524-4628

SUPPLEMENTAL MATERIAL

Supplemental methods

Description of cohort

The study sample was derived from a cohort of 97 acute ischemic stroke patients who received both DSC-MRI and rsfMRI between 2009 and 2015. Forty-seven patients showed no visible supratentorial hypoperfusion relevant to the acute infarct (on Tmax maps) and were excluded. Of the remaining fifty patients, 4 were excluded due to poor-quality DSC-MRI data (either because of severe motion or technical problems with contrast agent injection) and 11 had motion in their rsfMRI scans that exceeded predefined thresholds (framewise displacement between any two adjacent volumes > 3 mm or mean framewise displacement across the entire scan > 0.5 mm). Five more patients were excluded because of either subthreshold motion spikes (n = 3) or small but repetitive motion throughout the rsfMRI scan (n = 2) that clearly affected data quality (by causing a "striped" artifact in the images, for example). The remaining thirty patients were included in the final study sample.

Custom EPI template

This was created based on a previously described procedure[1]. Resting-state EPI datasets (mean across 150 volumes) from 103 stroke patients were registered to standard MNI space using FSL FLIRT (FMRIB's Linear Image Registration Tool, with 6 degrees-of-freedom) to place the images in the same orientation. The mean of these images (across patients) was used as an intermediate template, to which the original images were once again registered using an affine (12-degree-of-freedom) transformation. This procedure was performed three times and the output of the third iteration was the final EPI template.

Coregistration and CSF removal

First, the preprocessed DSC-MRI and rsfMRI data were registered to the subject-specific B0 image (in DWI space). Second, the B0 image was registered to the custom EPI template. By concatenating the transformation matrices from these two steps, the perfusion and BOLD delay maps were registered in one step to the custom EPI template. All image registration was performed with FSL FLIRT.

Cerebrospinal fluid (CSF) artifacts were removed from the perfusion maps using masks derived from segmented T2-weighted (B0) images (using FMRIB's Automated Segmentation Tool, FAST). By inverting the values in these masks and multiplying them by each of the perfusion maps, we preserved only those voxels outside the CSF. In addition, the lateral ventricle was extracted from the CSF masks (using a lateral ventricle template in standard space[2]), slightly expanded, had its values inverted, and was multiplied by the perfusion maps to remove artifacts immediately adjacent to the ventricles.

Vascular territory atlas and regions-of-interest

The vascular territory atlas (see below) was manually drawn based on published templates[3] in the custom EPI template space and covered the whole brain, excluding the brainstem and cerebellum. For the region-of-interest (ROI) analysis, each unique vascular territory on each slice (total = 156 per dataset) was used as a ROI to extract the mean values from the different perfusion maps.

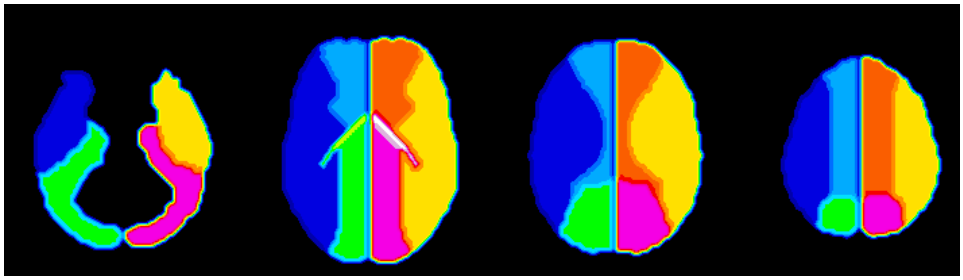

Venous sinus template

The venous sinus template (see below) was created from the post-gadolinium high-resolution T1-weighted (MPRAGE) scans of eight individuals. First, the brain was extracted and segmented into grey matter, white matter, and CSF using FSL BET and SPM8 respectively. These tissue masks were then combined and the result was subtracted from the brain-extracted T1 image, leaving an image containing only the vessels, which was registered to MNI space (0.5 mm). These images were binarized, the binarized masks of all subjects were added together then manually corrected to remove arteries, residual skull and other voxels outside the main venous sinuses (superior sagittal, inferior sagittal, straight, and transverse sinuses). The result was then spatially smoothed with a 0.5 mm Gaussian filter.

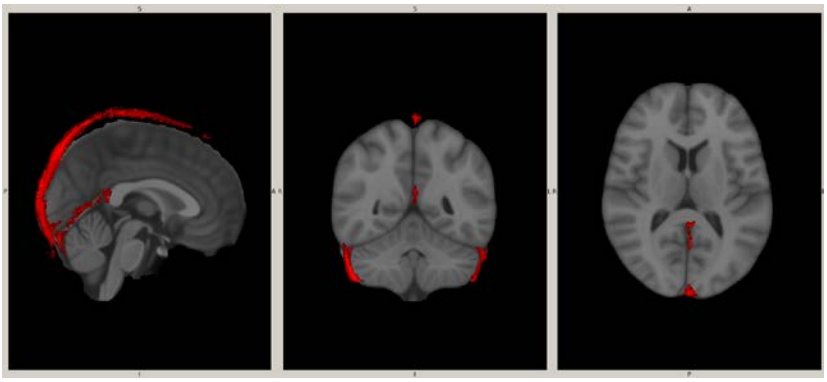

Supplemental figures and figure legends

Supplemental figure I

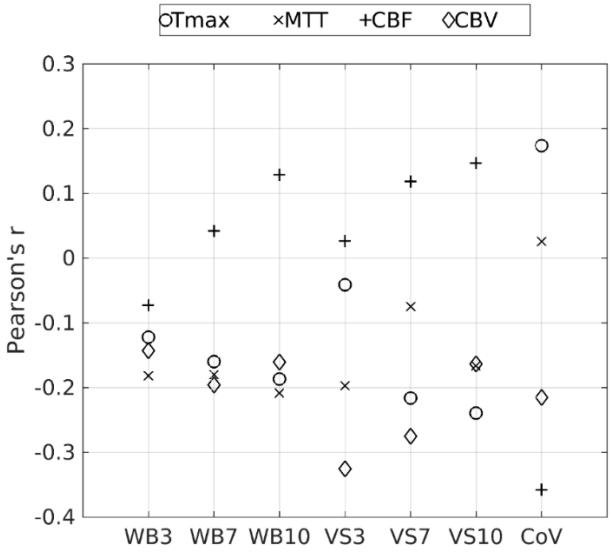

Correlation coefficients between mean framewise displacement and the strength of the (ROI-based) correlations between each of the DSC-MRI parameters and the BOLD-based parameters across the subjects in the cohort. Many of these are negative correlations, however, none are statistically significant ($p>0.05$).

Supplemental figure II

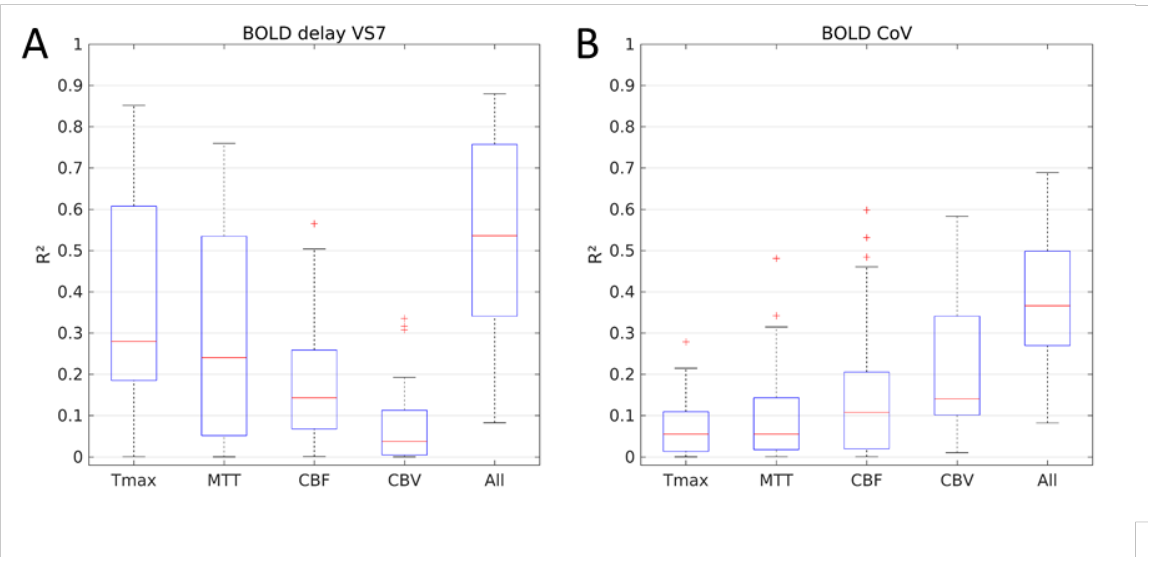

Boxplots of the values of R^2 across patients in the study sample (n=30). Each of the first four regression models included a single DSC-MRI parameter as an independent variable, with BOLD delay (A) and BOLD coefficient of variation (B) as the dependent variables. The "All" model incorporated all four DSC-MRI parameters together as independent variables.

Supplemental figure III

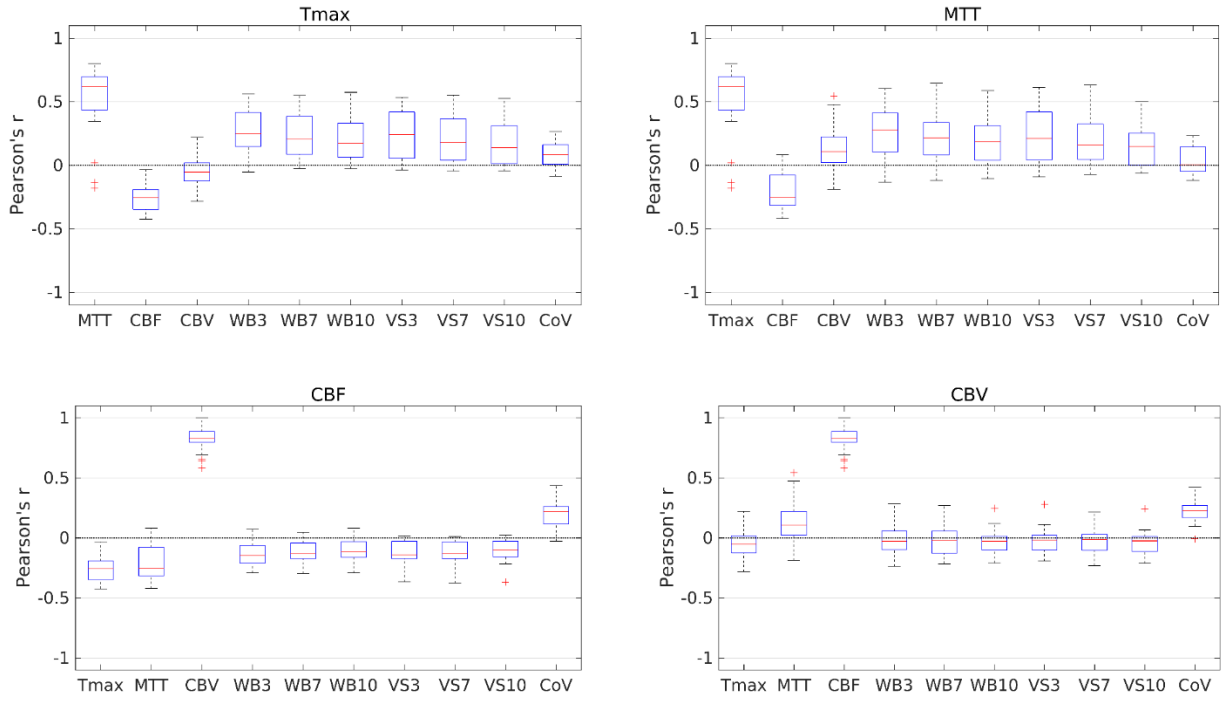

Boxplots of the correlation coefficients from the voxelwise comparison of the different perfusion maps for the study sample (n=30). WB = BOLD delay using whole-brain reference signal, VS = BOLD delay using venous reference signal, CoV = BOLD signal coefficient of variation.

Supplemental references

1. Fillmore PT, Phillips-Meek MC, Richards JE. Age-specific MRI brain and head templates for healthy adults from 20 through 89 years of age. Front. Aging Neurosci. 2015;7:44.

2. Kempton MJ, Underwood TSA, Brunton S, et al. A comprehensive testing protocol for MRI neuroanatomical segmentation techniques: Evaluation of a novel lateral ventricle segmentation method. Neuroimage 2011;58(4):1051–9.

3. Tatu L, Moulin T, Vuillier F, Bogousslavsky J. Arterial territories of the human brain. Front. Neurol. Neurosci. 2012;30:99–110.